

# **Geophysical Research Letters**°



# **RESEARCH LETTER**

10.1029/2023GL103154

#### **Key Points:**

- A new oceanic Ensemble Forecast Sensitivity to Observation (EFSO) is proposed and implemented on the CFSv2 to investigate observation impacts
- The 24-hr CFSv2 forecasts of sea temperature, salinity, and 2-m air temperature were improved by 1.5%, 0.8%, and 0.4%, respectively, after removing detrimental ocean observations detected by EFSO
- The improvements in the CFSv2 forecast can last for at least 5 days for the ocean and 3 days for the low-level atmosphere

#### **Supporting Information:**

Supporting Information may be found in the online version of this article.

#### Correspondence to:

C.-C. Chang, cchang75@umd.edu

#### Citation:

Chang, C.-C., Chen, T.-C., Kalnay, E., Da, C., & Mote, S. (2023). Estimating ocean observation impacts on coupled atmosphere-ocean models using Ensemble Forecast Sensitivity to Observation (EFSO). *Geophysical Research Letters*, 50, e2023GL103154. https://doi.org/10.1029/2023GL103154

Received 7 FEB 2023 Accepted 11 SEP 2023

#### **Author Contributions:**

**Conceptualization:** Tse-Chun Chen, Eugenia Kalnay

Funding acquisition: Eugenia Kalnay Project Administration: Eugenia Kalnay Software: Cheng Da

Supervision: Tse-Chun Chen, Eugenia

Writing – review & editing: Tse-Chun Chen, Cheng Da, Safa Mote

#### © 2023 The Authors.

This is an open access article under the terms of the Creative Commons Attribution-NonCommercial License, which permits use, distribution and reproduction in any medium, provided the original work is properly cited and is not used for commercial purposes.

# Estimating Ocean Observation Impacts on Coupled Atmosphere-Ocean Models Using Ensemble Forecast Sensitivity to Observation (EFSO)

Chu-Chun Chang<sup>1,2</sup>, Tse-Chun Chen<sup>3</sup>, Eugenia Kalnay<sup>1,4,5</sup>, Cheng Da<sup>6</sup>, and Safa Mote<sup>1,5,7</sup>

<sup>1</sup>Department of Atmospheric and Oceanic Science, University of Maryland, College Park, MD, USA, <sup>2</sup>Woodwell Climate Research Center, Falmouth, MA, USA, <sup>3</sup>Pacific Northwest National Laboratory, Richland, WA, USA, <sup>4</sup>Earth System Science Interdisciplinary Center, Cooperative Institute for Satellite Earth System Studies, College Park, MD, USA, <sup>5</sup>Institute for Physical Science and Technology, University of Maryland, College Park, MD, USA, <sup>6</sup>Earth System Science Interdisciplinary Center, University of Maryland, College Park, MD, USA, <sup>7</sup>Fariborz Maseeh Department of Mathematics and Statistics, Portland State University, Portland, OR, USA

**Abstract** Ensemble Forecast Sensitivity to Observation (EFSO) is a technique that can efficiently identify the beneficial/detrimental impacts of every observation in ensemble-based data assimilation (DA). While EFSO has been successfully employed on atmospheric DA, it has never been applied to ocean or coupled DA due to the lack of a suitable error norm for oceanic variables. This study introduces a new density-based error norm incorporating sea temperature and salinity forecast errors, making EFSO applicable to ocean DA for the first time. We implemented the oceanic EFSO on the CFSv2-LETKF and investigated the impact of ocean observations under a weakly coupled DA framework. By removing the detrimental ocean observations detected by EFSO, the CFSv2 forecasts were significantly improved, showing the validation of impact estimation and the great potential of EFSO to be extended as a data selection criterion.

**Plain Language Summary** This study introduces a new method to efficiently estimate the beneficial/detrimental impacts of each oceanic observation in the air-sea coupled data assimilation (CDA) by incorporating the forecast errors for sea temperature and salinity with a novel density norm. For the first time, we implemented this approach onto the operational-like CDA system and examined the impacts of ocean observations on the National Centers for Environmental Prediction CFSv2 forecasts. Our findings demonstrate that assimilating ocean profiles and satellite-retrieved sea surface temperature products significantly improves the CFSv2 forecasts. Moreover, after excluding the detrimental ocean observations identified by our new method, we observed significant improvements in the CFSv2 forecasts. This result validates the accuracy of impact estimation and underscores its great potential as a data selection criterion in CDA.

#### 1. Introduction

In numerical weather prediction, data assimilation (DA) is essential to enhance state estimation by optimally combining model forecasts and observations. The abundance of observations in recent years has significantly improved the analyses and forecasts through advanced state estimations. However, the growing number of observations from various platforms also heightens the need for techniques that can monitor the impact of individual observation in DA.

The Forecast Sensitivity to Observation (FSO) proposed by Langland and Baker (2004, hereafter LB04) is an advanced approach for estimating observation impact without conducting data-denial (with and without observations) experiments. FSO attributes the differences between the forecasts initialized with (e.g., from analysis) and without DA (e.g., from background) to individual observations using adjoint formulation, and it has been widely applied to variational DAs in operational and research centers (Cardinali, 2009; Lorenc & Marriott, 2014; Zhang et al., 2015; Zhu & Gelaro, 2008).

For the ensemble-based DA, Li et al. (2010) and Liu and Kalnay (2008) first introduced the Ensemble Forecast Sensitivity to Observation (EFSO) for the local ensemble transform Kalman filter (LETKF, Hunt et al., 2007). Unlike FSO, EFSO utilizes the ensemble information from DA instead of adjoint/tangent linear models, making it applicable to models without a tangent-linear model. Kalnay et al. (2012, hereafter K12) further refined the EFSO formulation, making it simpler and applicable to all ensemble Kalman filters (EnKFs). EFSO has

CHANG ET AL. 1 of 11

While EFSO has gained popularity in atmospheric DA, it has not been applied to ocean or coupled systems to the best of our knowledge. The development of oceanic EFSO faces two primary challenges: sparse observations and the absence of a suitable error norm. Unlike the atmosphere, the inherent scarcity of oceanic observations introduces greater uncertainties in the analyses, resulting in a reference state with larger uncertainties in oceanic EFSO than in atmospheric EFSO. This issue could potentially weaken the robustness of oceanic EFSO.

Oceanic EFSO requires an error norm that can incorporate forecast errors for salinity and sea temperature, which are fundamental and operationally assimilated variables in ocean models. The error norm aims to integrate comprehensive impacts in a single scalar, enabling the quantification of forecast errors for different variables using a unified unit in the EFSO. For example, the atmospheric EFSO commonly uses the dry and moist energy norms (Ehrendorfer et al., 1999) to encompass the forecast errors of key meteorological variables, such as wind, temperature, and surface pressure, into an energy term. In contrast, salinity lacks a direct association with a known energy term like atmospheric variables, posing a significant obstacle in oceanic EFSO development.

This study introduces a new oceanic EFSO by first addressing the error norm challenge. We propose a novel ocean density-based error norm that simultaneously incorporates sea temperature and salinity. The oceanic EFSO is implemented on the CFSv2-LETKF (Sluka, 2018), an atmosphere-ocean coupled system, to investigate the impacts of ocean observations within a weakly coupled DA (WCDA) framework (Penny et al., 2017; Penny & Hamill, 2017).

# 2. Model and Methodologies

#### 2.1. The CFSv2-LETKF System

The CFSv2-LETKF is an operational-like coupled DA system incorporating version two of the NCEP Climate Forecast System (CFSv2, Saha et al., 2010, 2014) and the LETKF (Hunt et al., 2007). The CFSv2 is a fully coupled atmosphere-ocean-land-sea ice model that provides global retrospective forecasts, reanalysis, and operational seasonal predictions. The NCEP GFS and the Geophysical Fluid Dynamics Laboratory Modular Ocean Model version 4 (MOM4, Griffies et al., 2004) perform atmosphere and ocean simulations, respectively. The 4-level Noah land surface model presents the land components as part of the GFS model with dynamic vegetation. A sea ice model (Winton, 2000) simulates ice dynamics, vertical thermodynamics, ice transport, and surface albedo.

The LETKF is employed to update the CFSv2 atmosphere and ocean ensembles. The CFSv2-LETKF consists of GFS-LETKF (Lien et al., 2013) and MOM-LETKF (Penny et al., 2013, 2015). The background error covariance of LETKF is estimated from CFSv2 forecast ensembles, presenting flow-dependent characteristics in its error statistics. For a coupled system, the state vector **x** includes atmosphere and ocean components. Namely,

$$\mathbf{x} = \left[ \mathbf{x}^{\text{ATM}} \ \mathbf{x}^{\text{OCN}} \right].$$

In the CFSv2-LETKF, the atmospheric analysis variables ( $\mathbf{x}^{\text{ATM}}$ ) are winds, air temperature, moisture, and surface pressure. The oceanic analysis variables ( $\mathbf{x}^{\text{OCN}}$ ) are sea temperature (T) and salinity (S). This study focuses on WCDA, where the  $\mathbf{x}^{\text{ATM}}$  and  $\mathbf{x}^{\text{OCN}}$  are updated independently with observations in their respective domains (Figure S2 in Supporting Information S1). Despite the absence of cross-domain increments in DA, changes made in one domain (e.g., ocean) can still influence the other domain (e.g., atmosphere) through coupled forecasting.

#### 2.2. The Ensemble Forecast Sensitivity to Observation (EFSO)

This section briefly introduces the EFSO formulation following K12. Detailed derivation and a schematic figure can be found in Text S1 and Figure S1 in Supporting Information S1. Here,  $\overline{\mathbf{x}_t^g}$  and  $\overline{\mathbf{x}_t^f}$  are the forecasts at time t

CHANG ET AL. 2 of 11

initialized from the background and the analysis at time 0, respectively. The corresponding forecast errors  $e_t^g$  and  $e_t^f$  are verified against the reference state  $\mathbf{x}_t^v$  at time t and can be represented as:

$$\boldsymbol{e}_{t}^{f} = \overline{\mathbf{x}_{t}^{f}} - \mathbf{x}_{t}^{v}, \boldsymbol{e}_{t}^{g} = \overline{\mathbf{x}_{t}^{g}} - \mathbf{x}_{t}^{v}. \tag{1}$$

This study uses the subsequent CFSv2 analysis as the reference state. Following LB04, the forecast error reduction (or increase)  $\Delta e^2$  is defined as:

$$\Delta e^{2} = e_{t}^{f T} C e_{t}^{f} - e_{t}^{g T} C e_{t}^{g} = (e_{t}^{f} - e_{t}^{g})^{T} C (e_{t}^{f} + e_{t}^{g})$$

$$\approx \left[ \mathbf{M} \left( \overline{\mathbf{x}}_{0}^{a} - \overline{\mathbf{x}}_{0}^{b} \right) \right]^{T} C (e_{t}^{f} + e_{t}^{g}) = \left[ \mathbf{M} \mathbf{K} \delta \mathbf{y}_{o} \right]^{T} C (e_{t}^{f} + e_{t}^{g}).$$
(2)

The superscripts a and b represent the analysis and background, respectively.  $\overline{\mathbf{x}^{(\cdot)}}$  is the ensemble mean.  $\delta \mathbf{y}_o = \mathbf{y}_0 - \mathbf{H}\left(\overline{\mathbf{x}_0^b}\right)$ , where  $\mathbf{y}_o$  denotes observations, and  $\mathbf{H}$  is the linear observation operator.  $\mathbf{M}$  represents the tangent linear forecast model (TLM), and  $\mathbf{K}$  is the Kalman gain.  $\mathbf{C}$  is the forecast error norm.

K12 extends the adjoint-based cost function (Equation 2) to a simpler, TLM-free form for ensemble-based DA by assuming  $\mathbf{K} = \left(\frac{1}{k-1}\right) \mathbf{X}_0^a \mathbf{X}_0^{a^{\mathrm{T}}} \mathbf{H}^{\mathrm{T}} \mathbf{R}^{-1}$  and  $\mathbf{X}_t^b \approx \mathbf{M} \mathbf{X}_0^a$ , where  $\mathbf{X}^{(\cdot)}$  represents the perturbation departure from the mean state, and k is the ensemble size. Thus, Equation 2 becomes (Equation 6 in K12):

$$\left(\Delta e^{2}\right)^{\text{EFSO}} = \left(\frac{1}{k-1}\right) \delta \mathbf{y}_{o}^{T} \left[\rho^{\circ} \mathbf{R}^{-1} (\mathbf{H} \mathbf{X}_{0}^{a}) \mathbf{X}_{t}^{bT} \mathbf{C} \left(\mathbf{e}_{t}^{f} + \mathbf{e}_{t}^{g}\right)\right],\tag{3}$$

where **R** is the observation error covariance.  $(\Delta e^2)^{\text{EFSO}}$  is the EFSO estimation, where a negative (positive) sign represents the beneficial (detrimental) observation for the forecast verified at time t.  $\rho$  is the localization matrix whose row is the weighting for each observation, and the symbol  $^{\circ}$  denotes the element-wise multiplication (Schur product).

The EFSO can be estimated by different error norms. For oceanic EFSO, we propose an ocean density norm that naturally incorporates the forecast error reductions for the dominant prognostic ocean variables T and S:

$$e^{T}Ce = \frac{1}{2} \frac{1}{L} \int_{L} \int_{z} d'(T, S, z, \theta)^{2} dz dL,$$
(4)

where d' denotes the perturbation of the converted ocean density. L is the target region. The density conversion is conducted using the Thermodynamic Equation of Seawater-2010 (TEOS-10, McDougall & Barker, 2011), where functions involving ocean T, S, latitude ( $\theta$ ), and vertical ocean depth (z) are applied to estimate the density perturbation. The detailed conversion process using TEOS-10 is described in Text S2 in Supporting Information S1.

#### 3. Experimental Design

Our model configuration closely follows the operational CFSv2 (Saha et al., 2010). The atmosphere model resolution is spectral T126 ( $\sim$ 1°) with 64 vertical levels (up to 0.02 hPa). The ocean model has 40 vertical subsurface layers with a resolution of 10 m near the surface (top layer at 5 m), and the horizontal resolution is 0.25° near the equator (10°S to 10°N latitude band) and 0.5° elsewhere.

The 40 ensembles were initialized from the NCEP CFS Reanalysis (CFSR) and a 4-month free run was conducted to establish sufficient ensemble spread. Then, a 2-month DA cycling was carried out from 00 UTC 1 January 2010 as a spin-up, followed by the 1-month experiments from 00 UTC 1 March to 18 UTC 31 March 2010. The flowchart of the experiment is in Figure S3 in Supporting Information S1.

We assimilated the conventional data (e.g., no radiance, GPS radio occultation, and precipitation data) from the NCEP PREPBUFR every 6 hr (00, 06, 12, 18Z) for the atmosphere. For ocean DA, the NOAA Geo-Polar Blended level-4 Sea Surface Temperature (L4SST) (Maturi et al., 2017) with 0.25° resolution (~27 km) and the ocean T and S profiles from the World Ocean Database (Boyer et al., 2013) were assimilated daily at 12Z.

Localizations were applied using a compactly supported fifth-order piecewise function (Equation 4.10 in Gaspari & Cohn, 1999) with a horizontal length scale of 500 km and a vertical e-folding scale of 0.4 scale height for

CHANG ET AL. 3 of 11

The oceanic EFSO values were estimated daily at 12Z, with subsequent analyses serving as the reference state. The evaluation forecast length is 24 hr. Due to the relatively short timescale, lower resolution, and limited representation of the surface ocean dynamics in the CFSv2, the moving localization in K12 for ocean current motions (e.g., at approximately 10 cm/s) is not necessary for this study. However, in reality, the strength of currents can be an order of magnitude larger in certain regions, and these currents can present meandering behavior from hour to hour, leading to wider fluctuations in current speed at specific locations. Thus, models that simulate fine ocean surface conditions should consider incorporating moving localization to reflect real-world situations accurately.

#### 4. Results

# 4.1. Geographical Impacts of Satellite SST and Ocean Profiles

This section investigates the geographical significance and relative importance of L4SST and ocean profiles using EFSO. The L4SST are globally and uniformly distributed data, making them ideal for illustrating the geographical significance of ocean observation impacts near the surface. On the other hand, ocean profiles consist of diverse in situ measurements from sources like buoys, Argo floats, and ships, which are more abundant in the Tropics, coastal regions, and along ocean currents, as shown in Figures 1b and 1c. The vertical impacts of ocean profiles are further discussed in Section 4.2.

Figure 1 shows the monthly-mean EFSO estimation for L4SST (Figure 1a) and the snapshots of the EFSO estimations for T (Figure 1b) and S (Figure 1c) profiles per assimilated observation. First, the averaged negative EFSO values indicate that assimilating L4SST and profiles benefits the CFSv2 forecast. Second, areas with higher climate variabilities, such as the eastern equatorial Pacific Ocean, the Gulf Stream in the Atlantic Ocean, and the Kuroshio Current in the North Pacific, exhibit more significant observation impacts (Figure 1). That is attributed to the larger uncertainties (e.g., ensemble spread) in these areas, which leads to more substantial corrections from observations during DA.

Notably, two cyclonic (TC) features in the southwestern Pacific Ocean, associated with the TCs Tomas and Ului (2010), represent substantial EFSO values (Figure 1a). Storm activities can induce upper ocean perturbations through thermal (e.g., latent heat fluxes from evaporations and precipitation) and dynamic (e.g., turbulent mixing by surface winds) processes, resulting in notable error fluctuations in the ocean state (Bueti et al., 2014; Emanuel, 2001; Sriver et al., 2010). As a consequence, larger EFSO values emerge along storm tracks. This finding highlights the significance of air-sea interactions between the upper ocean and TCs on ocean DA, even within a WCDA framework. Therefore, ocean observations along storm tracks and in areas with high SST variability hold greater influence for DA, and the presence of TCs should be considered when designing future ocean observing systems. An illustration of how SST observation impacts may vary during TC events is presented in Text S5 in Supporting Information S1.

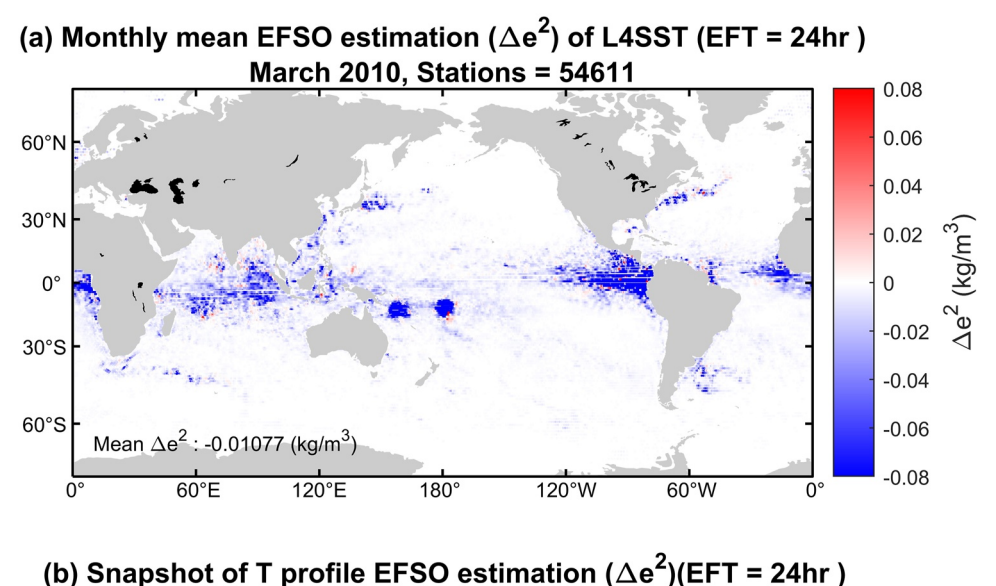
# 4.2. The Vertical Characteristics of Ocean Observation Impacts

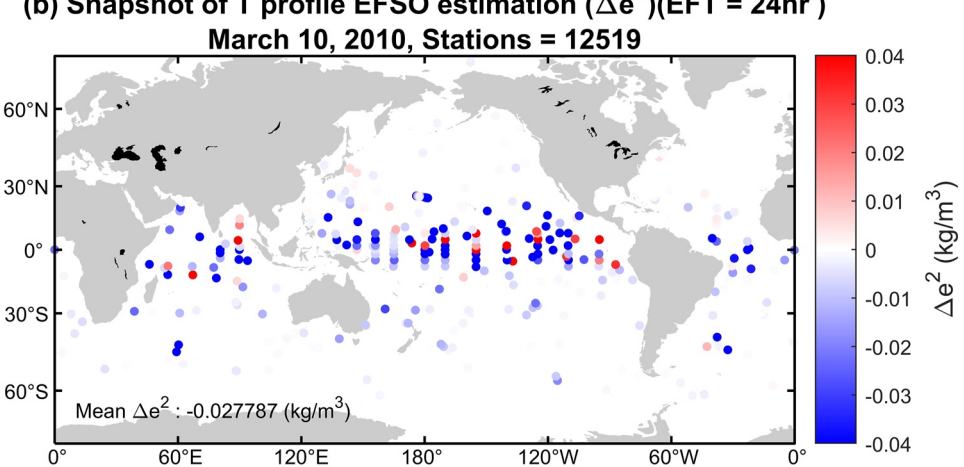
The ocean T and S profiles consist of multi-platform observations collected at various depths and locations in the ocean, spanning from the surface to over 1000 m depth. However, the majority of these profiles (>75%) are within the mixed layer (Figures 2a and 2d). For simplicity, we define the mixed layer as the top 200 m of the ocean, as a globally averaged thickness, although its thickness can vary with seasons and location.

Figures 2b and 2e are the zonal mean EFSO estimation per observation of T and S profiles. The negative mean EFSO values suggest assimilating the profiles benefits all ocean levels. However, the observation impacts vary based on latitudes and depths. The most significant impacts are within the tropical mixed layer (Figures 2b and 2e) due to the more active dynamics in that region, such as increased flux exchanges, mixings, wind-driven turbulence, and storm activities. These factors contribute to significant variations in forecast errors, resulting in larger EFSO estimations.

CHANG ET AL. 4 of 11

19448007, 2023, 20, Downloaded from https://agupubs.onlinelibrary.wiley.com/doi/10.1029/2023GL103154 by Portland State University, Wiley Online Library on [08.03:2024]. See the Terms and Conditions (https://onlinelibrary.wiley





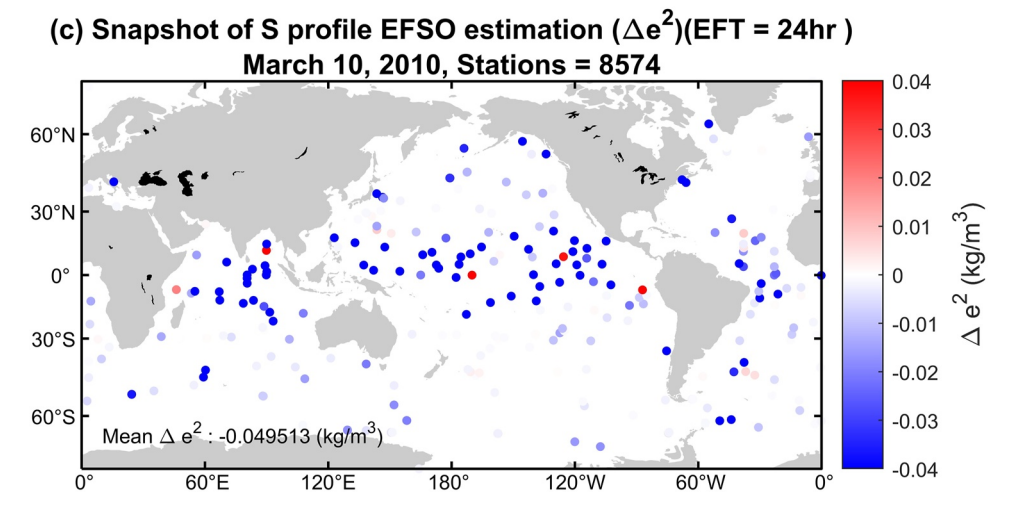


**Figure 1.** Geographical distribution of (a) the monthly-mean Ensemble Forecast Sensitivity to Observation (EFSO) of level-4 Sea Surface Temperature (L4SST) and the snapshots of EFSOs of the (b) T and (c) S profiles on 10 March 2010. The corresponding EFSO for each observation is shown with colors, where blue (red) represents beneficial (detrimental) impacts. For the ocean profiles, the displayed values are the EFSO estimations of the entire water column.

CHANG ET AL. 5 of 11

19448007, 2023, 20, Downloaded from https://agupubs.onlinelibrary.wiley.com/doi/10.1029/2023GL103154 by Portland State University, Wiley Online Library on [08/03/2024]. See the Terms and Conditions (https://agupubs.onlinelibrary.wiley.com/doi/10.1029/2023GL103154 by Portland State University, Wiley Online Library on [08/03/2024]. See the Terms and Conditions (https://agupubs.onlinelibrary.wiley.com/doi/10.1029/2023GL103154 by Portland State University, Wiley Online Library on [08/03/2024]. See the Terms and Conditions (https://agupubs.onlinelibrary.wiley.com/doi/10.1029/2023GL103154 by Portland State University, Wiley Online Library on [08/03/2024]. See the Terms and Conditions (https://agupubs.onlinelibrary.wiley.com/doi/10.1029/2023GL103154 by Portland State University, Wiley Online Library on [08/03/2024]. See the Terms and Conditions (https://agupubs.onlinelibrary.wiley.com/doi/10.1029/2023GL103154 by Portland State University, Wiley Online Library on [08/03/2024]. See the Terms and Conditions (https://agupubs.onlinelibrary.wiley.com/doi/10.1029/2023GL103154 by Portland State University, Wiley Online Library on [08/03/2024]. See the Terms and Conditions (https://agupubs.onlinelibrary.wiley.com/doi/10.1029/2023GL103154 by Portland State University, Wiley Online Library on [08/03/2024]. See the Terms and Conditions (https://agupubs.onlinelibrary.wiley.com/doi/10.1029/2023GL103154 by Portland State University, Wiley Online Library on [08/03/2024]. See the Terms and Conditions (https://agupubs.onlinelibrary.wiley.com/doi/10.1029/2023GL103154 by Portland State University, Wiley Online Library on [08/03/2024]. See the Terms and Conditions (https://agupubs.onlinelibrary.wiley.com/doi/10.1029/2023GL103154 by Portland State University, Wiley Online Library on [08/03/2024]. See the Terms and Conditions (https://agupubs.onlinelibrary.wiley.com/doi/10.1029/2023GL103154 by Portland State University (https://agupubs.onlinelibrary.wiley.com/doi/10.1029/2023GL103154 by Portland State University (https://agupubs.onlinelibra

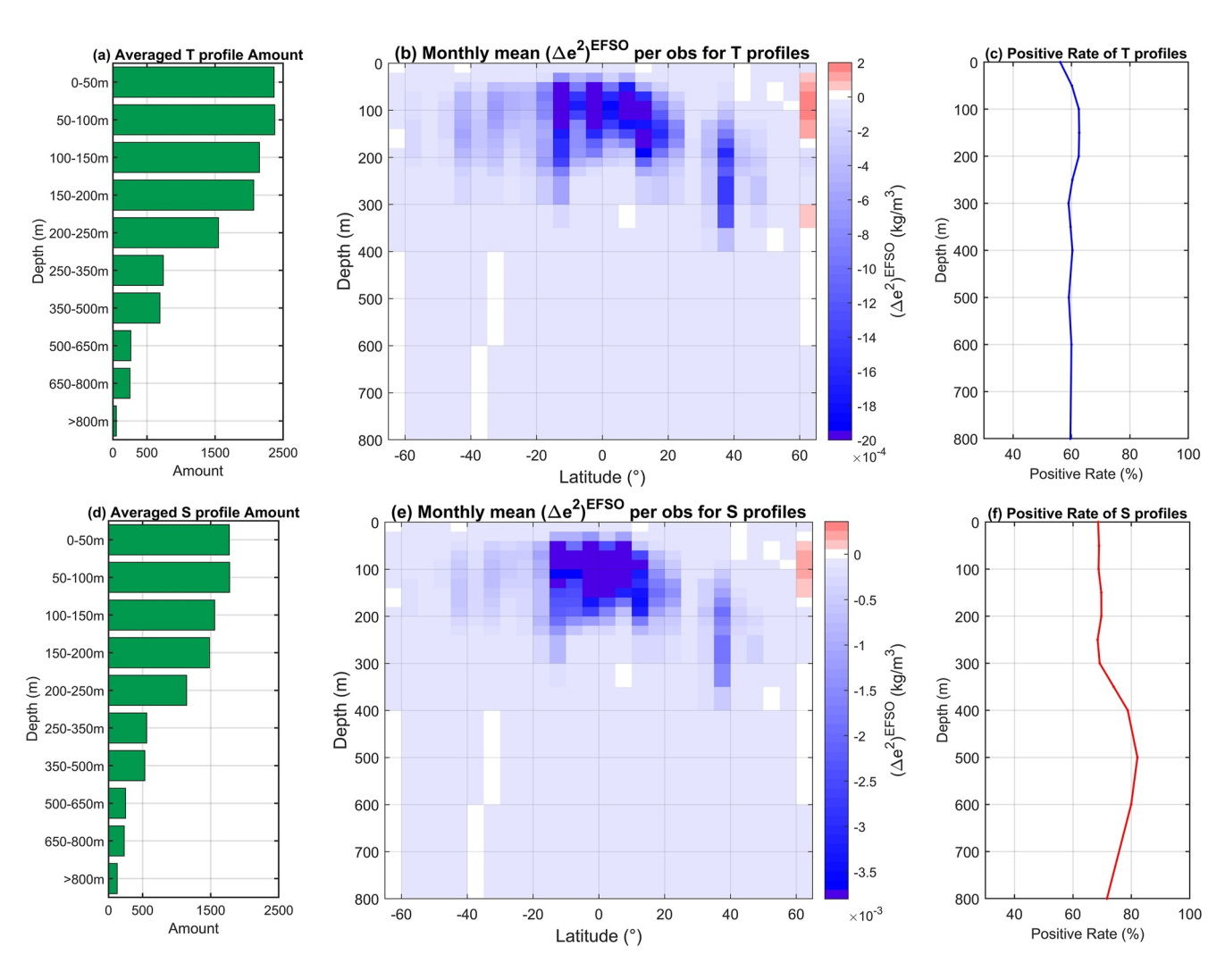


Figure 2. The monthly mean of the (a, d) observation amounts, (b, e) the zonal-mean Ensemble Forecast Sensitivity to Observation (EFSO) estimations, and (c, f) the positive rate with respect to ocean depths. Variables shown here are the ocean T (a, b, c) and S profiles (d, e, f).

Noticeable EFSO impacts are also observed in areas linked to deep-water formation and water mixing around 40°N (Figures 2b and 2e). Here, the Kuroshio Current and the Atlantic meridional overturning circulation contribute to substantial T and S gradients (Wang et al., 2010, Figures 1 and 2) (Figure S6 in Supporting Information S1), resulting in considerable density variations and, consequently, more significant observation impacts.

Furthermore, we observed slight degradations in the upper ocean above 65°N (highlighted in red in Figures 2b and 2e). That is possibly due to the presence of sea ice, which leads to more complex density conversion. As this study employs a density norm based on seawater, further investigations into sea ice EFSO would be needed.

Figures 2c and 2f are the positive rates of T and S profiles, respectively. Additional time series of the positive rates is shown in Figure S4 in Supporting Information S1. The positive rate is the percentage of the beneficial observation amount among all assimilated observations. The positive rates are approximately 60% for T profile and around 70% for S profile and are not sensitive to depth changes. This result aligns with Hotta et al. (2017), who found positive rates ranging from 55% to 74% for atmospheric observations in the GFS.

#### 4.3. Fixed Versus Non-Fixed Ocean Observations

Ocean profiles can be broadly categorized as fixed and non-fixed types. Fixed observations, like moored buoys, are anchored at specific locations. Non-fixed observations, such as drifters and floats, drift with ocean currents and even move vertically between the surface and a mid-water level. Figure 3a shows the observation locations, and

CHANG ET AL. 6 of 11

19448007, 2023, 20, Downloaded from https://agupubs.onlinelibrary.wiley.com/doi/10.1029/2023GL103154 by Portland State University, Wiley Online Library on [08/03/2024]. See the Terms

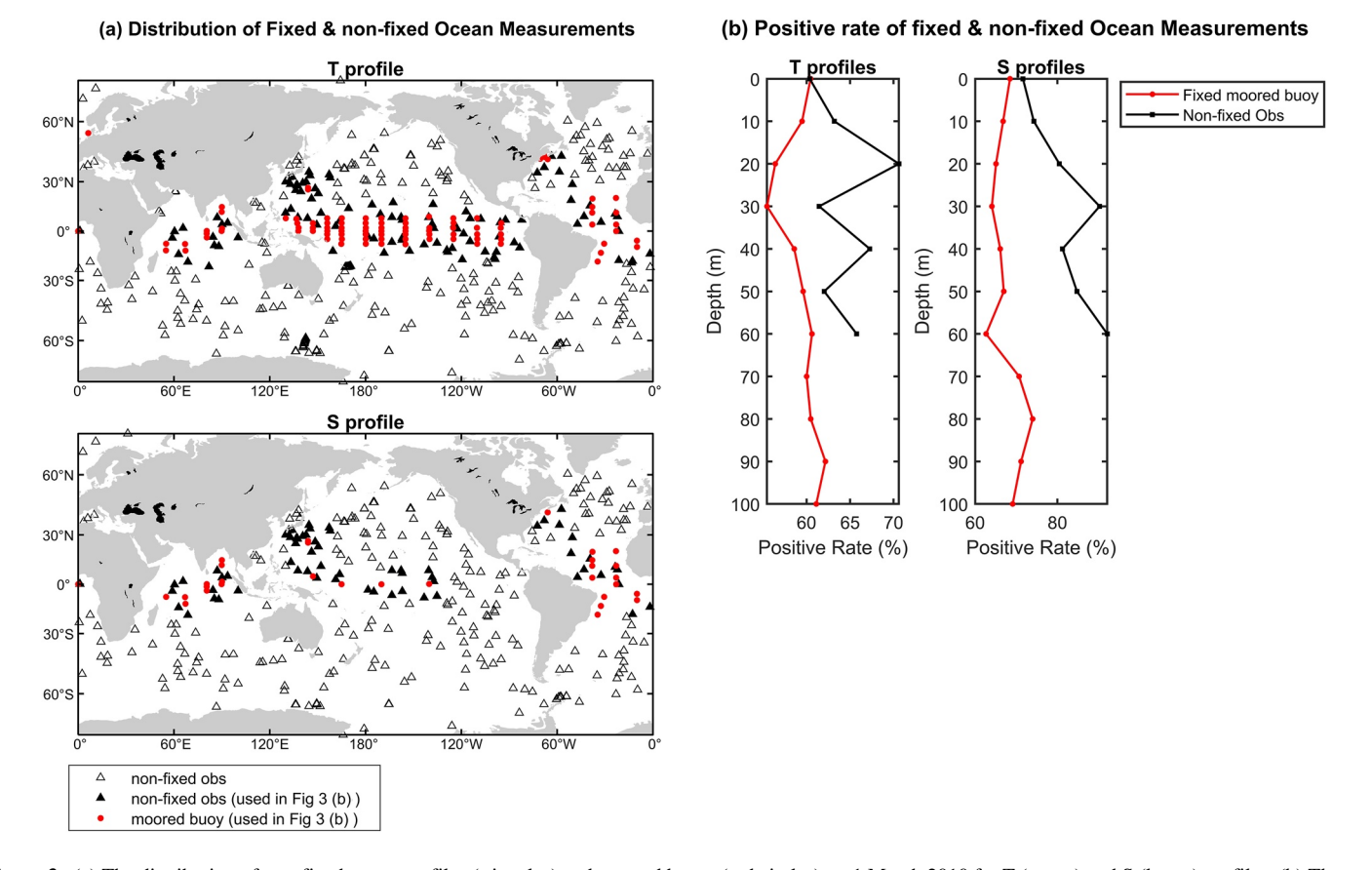


Figure 3. (a) The distribution of non-fixed ocean profiles (triangles) and moored buoys (red circles) on 1 March 2010 for T (upper) and S (lower) profiles. (b) The vertical distribution of the monthly-mean positive rate of the moored buoy (red) and non-fixed profiles (black) for T (left) and S (right) profiles.

Figure 3b compares their averaged beneficial rates. To ensure a fair comparison, we specifically compared the moored buoys with their adjacent non-fixed observations (black triangle in Figure 3a), excluding the potential impact due to different geographic locations. Details can be found in Text S3 in Supporting Information S1.

We found that the beneficial rate of the fixed moored buoy is consistently lower than the non-fixed observations, indicating that assimilating moored buoys yields less beneficial impacts than assimilating non-fixed observations. This finding aligns with Sivareddy et al. (2017), who found that assimilating moored buoys could potentially degrade the CFSv2 ocean analysis. A brief explanation of the cause is in Text S3 in Supporting Information S1.

It is worth noting that Sivareddy et al. (2017) draw the conclusion from conducting multiple trial-and-error experiments. In contrast, we discovered the same phenomena with solely one experiment using EFSO, which clearly demonstrates the efficiency of EFSO in monitoring the observation impacts on DA.

We want to emphasize that EFSO estimation is not necessarily equivalent to the intrinsic quality of observation, as it depends on both the backgrounds and observations (Chen & Kalnay, 2020; Hotta et al., 2017; Lien et al., 2018). Thus, the relatively lower beneficial impact observed for moored buoys should not be interpreted as flaws in the instrument.

# 4.4. Data-Denial Experiments

To validate the oceanic EFSO estimation and explore its potential in improving CFSv2 forecasts, we conducted a 1-month offline (e.g., non-cycled) data-denial experiment. At each ocean analysis time (e.g., daily at 12Z), a new analysis was generated by assimilating only the beneficial ocean observations identified by EFSO. Then, we compared its subsequent forecasts with the original ones. The variables examined here are ocean T, S, and atmospheric 2-m temperature (T2m). The ocean T and S forecasts were verified with ocean profiles, and the atmospheric T2m forecast was evaluated with the European Centre for Medium-Range Weather Forecasts reanalysis v5 (ERA5). Given that approximately 90% of rejected ocean observations were located above 250 m depth (Figures 4a and 4b), we expected most forecast improvements to occur in the upper ocean.

CHANG ET AL. 7 of 11

19448007, 2023, 20, Downloaded from https://agupubs.onlinelibrary.wiley.com/doi/10.1029/2023GL103154 by Portland State University, Wiley Online Library on [08/03/2024]. See the Terms and Conditions (https://onlinelibrary.wiley

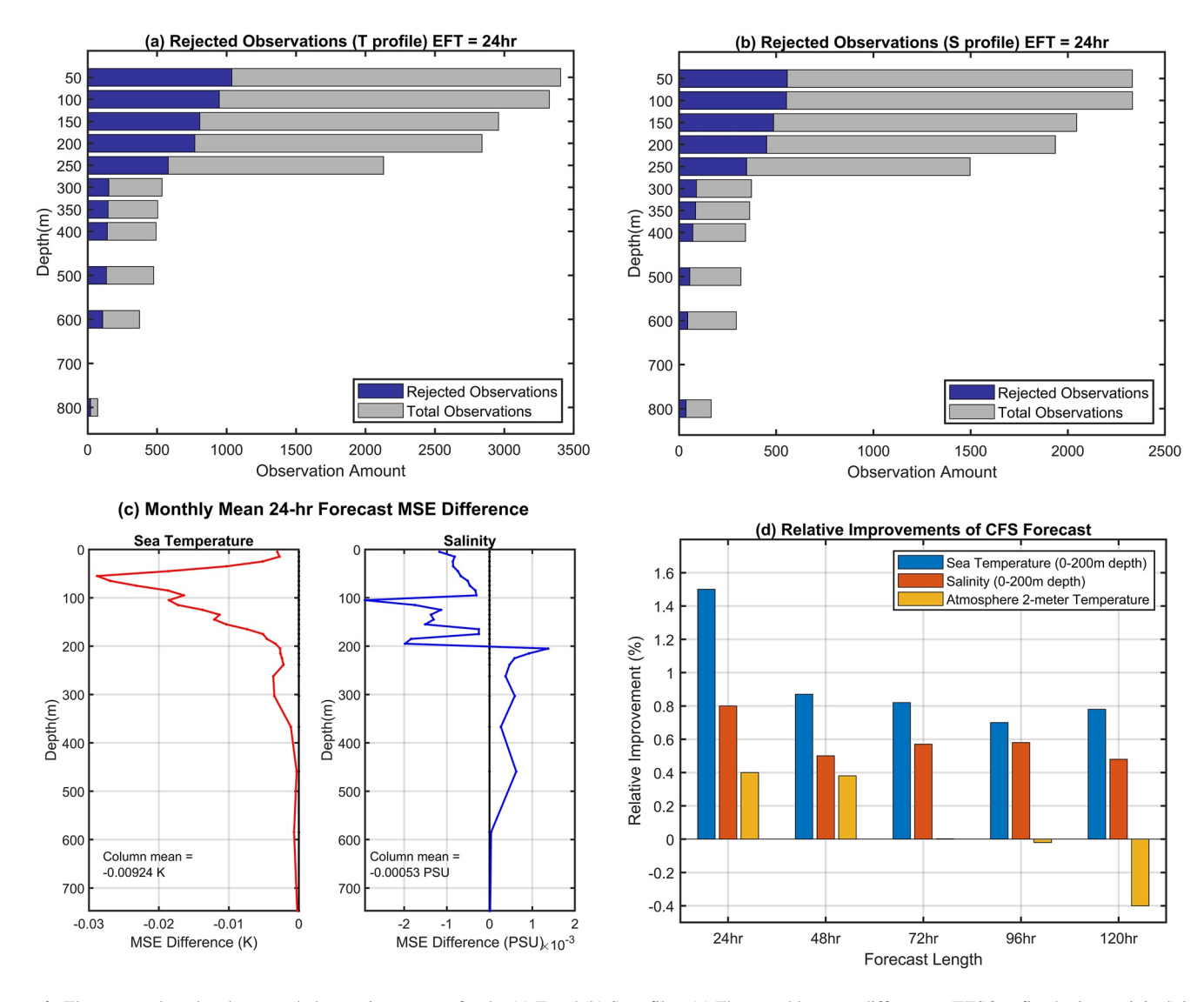


Figure 4. The averaged total and removed observation amount for the (a) T and (b) S profiles. (c) The monthly-mean differences (EFSO-refined minus original) in mean-squared errors (MSE) of the 24-hr forecasts. (d) The monthly-mean relative forecast improvement (%) of the ocean T (blue), S (red) in the mixed layer, and the atmosphere T2m (yellow) forecasts.

Figure 4c shows the monthly mean squared error differences between the EFSO-refined and original forecasts. As expected, most improvements occur within the mixed layer. The T forecasts for all levels significantly improved by removing detrimental observations (Figure 4c). In contrast, the S forecast was notably improved within the mixed layer but slightly degraded in the thermocline. A potential cause is the scarcity of S observations after data removal. Removing an excessive number of observations simultaneously in the thermocline may negatively impact the salinity analysis, especially given the limited number of S observations available. Hotta et al. (2017) have shown that removing all the detrimental observations does not guarantee the best result. Moreover, removing one observation may benefit one variable while being detrimental to another. This effect is more pronounced in the thermocline than in the mixed layer due to the strong correlation between T and S in the thermocline. Despite the slight degradation in thermocline S, noticeable improvement remains apparent in the mean S forecast for the entire water column.

Finally, we extended the CFSv2 forecast to 5 days and evaluated the relative forecast improvement (hereafter RFI), which is calculated as:

relative forecast improvement (RFI) = 
$$\frac{e_{\text{original}}^{f} - e_{\text{new}}^{f}}{e_{\text{original}}^{f}} \times 100\%.$$

CHANG ET AL. 8 of 11

where the  $e_{\text{new}}^f$  and  $e_{\text{original}}^f$  are the error of the forecasts initialized from the EFSO-refined and original analyses. So, a positive RFI means the EFSO-refined forecast is more accurate than the original, and vice versa. Figure 4d shows the monthly mean RFI of the mixed layer T and S, and the T2m, for the CFSv2 5-day forecasts. It is impressive that the EFSO-refined improvements last for at least 5 days for CFSv2 ocean forecasts and 2 days for the atmosphere T2m forecast. This result demonstrates that the improvements in the ocean state can affect the atmosphere through air-sea flux exchanges, consequently enhancing the CFSv2 forecasts (Figure S7 in Supporting Information S1).

The degradation of T2m forecasts over 72 hr may result from the ocean data selection strategy. In an alternative experiment, we removed observations with detrimental EFSO values exceeding five standard deviations ( $\sim$ 2% of all observations) instead of removing all. This adjustment leads to less pronounced RFI in both the ocean and atmosphere. However, it extended the beneficial impact on T2m forecasts, sustaining improvements for up to 96 hr (Figure S8 in Supporting Information S1).

This result suggests that certain ocean observations may negatively affect ocean density while benefiting the atmosphere, highlighting the importance of considering atmospheric impacts when applying quality control to ocean observations in a coupled system, even within WCDA. Further in-depth investigations are needed for a comprehensive understanding and to provide insights into optimizing the data selection strategy.

## 5. Summary and Discussion

This study introduces a novel density-based norm for oceanic EFSO and applies it to the operational-like CFSv2-LETKF. We explore ocean observation impacts within the WCDA framework and validate the impact estimation and feasibility of enhancing CFSv2 forecasts through a 1-month data-denial experiment. Our results demonstrate that oceanic EFSO can effectively identify the impact of each ocean observation, including L4SST and ocean profiles. Key findings include:

- 1. Ocean observations in the regions with higher variabilities, ocean current overturning, mixed water areas, and storm tracks have more significant impacts and can be more useful for DA.
- 2. The EFSO positive rate for non-fixed observations is consistently higher than for moored buoys, agreeing with Sivareddy et al. (2017) that assimilating moored buoys may instead degrade the CFS ocean analysis.
- 3. The CFSv2 forecasts significantly improved by removing detrimental ocean observations detected by EFSO. The improvements in the forecasts can last at least 5 days for the ocean and 2 days for the lower atmosphere.

Encouraged by these results, potential future directions for oceanic EFSO applications are proposed. First, it is promising to extensively apply oceanic EFSO as a data selection strategy (e.g., PQC, Hotta et al., 2017) to improve CFSv2 analysis and forecasts. Second, extending the density norm to an ocean energy norm that incorporates impacts related to ocean height is worth exploring (Text S3 in Supporting Information S1). This approach aligns the unit of ocean energy norm with the atmospheric energy norm, allowing EFSO to be applied with strongly coupled DA (SCDA). However, more investigations would be needed to adapt EFSO to SCDA.

Another future direction is applying EFSO to advanced ocean models with more explicit simulation of surface ocean dynamics and coupling effects. The CFSv2 model used in this study has limitations in representing sea surface and boundary dynamics due to its low resolution and absence of wave models. One potential approach is employing the proposed energy norm (Text S3 in Supporting Information S1) to account for forecast errors in T, S, and sea surface height, thereby considering changes in ocean currents.

Finally, exploring a novel extension for EFSO to adapt to advanced coupled data assimilation (CDA), such as the Ensemble Tangent Linear Model (ETLM, Bishop et al., 2017), is essential. ETLM uses ensemble information to calculate TLM, largely enhancing the feasibility of variational CDA. Strategies for incorporating EFSO into advanced CDA approaches like ETLM would be another exciting topic for future exploration.

# **Data Availability Statement**

The CFSv2-LETKF (Sluka, 2018) code is available at https://github.com/UMD-AOSC/CFSv2-LETKF. The TEOS-10 tool (McDougall & Barker, 2011) can be downloaded here: https://www.teos-10.org/software.htm#1 (version 3.05). The CFSR (Saha et al., 2010) data can be found: https://www.ncei.noaa.gov/access/metadata/

CHANG ET AL. 9 of 11

19448007, 2023,

landing-page/bin/iso?id=gov.noaa.ncdc:C00765. The NOAA GHRSST (Maturi, 2014; Maturi et al., 2017) are from: https://www.star.nesdis.noaa.gov/pub/socd2/coastwatch/sst\_blended/sst5km/night/ghrsst/.

#### Acknowledgments

We thank Dr. Travis Sluka for kindly providing the source code of CFSv2-LETKF. This work is supported by the National Oceanic and Atmospheric Administration (Grant NA14NES4320003) and the Monsoon Mission Project of the Indian Institute of Tropical Meteorology, Ministry of Earth Sciences (MoES), Government of India. Eugenia Kalnay and Safa Mote were supported by the Monsoon Mission II (Grant IITMMMIIU-NIVMARY-LANDUSA2018INT1), provided by the Ministry of Earth Science, India, and NOAA Cooperative Institutes (award no. NA19NES4320002), at the Cooperative Institute for Satellite Earth System Studies, under the project "Advanced EFSO-Based QC Methods for Operational Use and Agile Implementation of New Observing Systems." SM also acknowledges National Science Foundation RTG grant DMS-2136228. We extend our sincere gratitude to Dr. Steve Penny and the anonymous reviewer for their invaluable and insightful suggestions, which have significantly enhanced the quality and clarity of this paper.

## References

- Bishop, C. H., Frolov, S., Allen, D. R., Kuhl, D. D., & Hoppel, K. (2017). The local ensemble tangent linear model: An enabler for coupled model 4D-Var. *Quarterly Journal of the Royal Meteorological Society*, 143(703), 1009–1020. https://doi.org/10.1002/qj.2986
- Boyer, T. P., Antonov, J. I., Baranova, O. K., Coleman, C., Garcia, H. E., Grodsky, A., et al. (2013). World Ocean Database 2013. In S. Levitus (Ed.), & A. Mishonov, (Technical Ed.), NOAA Atlas NESDIS 72 (pp. 209). https://doi.org/10.7289/V5NZ85MT
- Bueti, M. R., Ginis, I., Rothstein, L. M., & Griffies, S. M. (2014). Tropical cyclone–induced thermocline warming and its regional and global impacts. *Journal of Climate*, 27(18), 6978–6999. https://doi.org/10.1175/JCLI-D-14-00152.1
- Cardinali, C. (2009). Monitoring the observation impact on the short-range forecast. Quarterly Journal of the Royal Meteorological Society, 135(638), 239–250. https://doi.org/10.1002/qj.366
- Chen, T. C., & Kalnay, E. (2020). Proactive quality control: Observing system experiments using the NCEP global forecast system. *Monthly*
- Weather Review, 148(9), 3911–3931. https://doi.org/10.1175/MWR-D-20-0001.1

  Ehrendorfer, M., Errico, R. M., & Raeder, K. D. (1999). Singular-vector perturbation growth in a primitive equation model with moist physics.
- Journal of the Atmospheric Sciences, 56(11), 1627–1648. https://doi.org/10.1175/1520-0469(1999)056<1627:SVPGIA>2.0.CO;2 Emanuel, K. (2001). Contribution of tropical cyclones to meridional heat transport by the oceans. Journal of Geophysical Research, 106(D14), 14771–14781. https://doi.org/10.1029/2000JD900641
- Gaspari, G., & Cohn, S. E. (1999). Construction of correlation functions in two and three dimensions. Quarterly Journal of the Royal Meteoro-
- logical Society, 125(554), 723–757. https://doi.org/10.1002/qj.49712555417
  Griffies, S. M., Harrison, M. J., Pacanowski, R. C., & Rosati, A. (2004). A technical guide to MOM4. GFDL Ocean Group Technical Report, 5,
- 342–371. Retrieved from https://www.gfdl.noaa.gov/bibliography/related\_files/smg0301.pdf
  Hotta, D., Chen, T. C., Kalnay, E., Ota, Y., & Miyoshi, T. (2017). Proactive QC: A fully flow-dependent quality control scheme based on EFSO.
- Monthly Weather Review, 145(8), 3331–3354. https://doi.org/10.1175/MWR-D-16-0290.1

  Hunt, B. R., Kostelich, E. J., & Szunyogh, I. (2007). Efficient data assimilation for spatiotemporal chaos: A local ensemble transform Kalman
- filter. Physica D: Nonlinear Phenomena, 230(1–2), 112–126. https://doi.org/10.1016/j.physd.2006.11.008
- Kalnay, E., Ota, Y., Miyoshi, T., & Liu, J. (2012). A simpler formulation of forecast sensitivity to observations: Application to ensemble Kalman filters. *Tellus A: Dynamic Meteorology and Oceanography*, 64(1), 18462. https://doi.org/10.3402/tellusa.v64i0.18462
- Kotsuki, S., Kurosawa, K., & Miyoshi, T. (2019). On the properties of ensemble forecast sensitivity to observations. Quarterly Journal of the Royal Meteorological Society, 145(722), 1897–1914. https://doi.org/10.1002/qj.3534
- Langland, R. H., & Baker, N. L. (2004). Estimation of observation impact using the NRL atmospheric variational data assimilation adjoint system. Tellus A: Dynamic Meteorology and Oceanography, 56(3), 189–201. https://doi.org/10.3402/tellusa.v56i3.14413
- Li, H., Liu, J., & Kalnay, E. (2010). Correction of 'Estimating observation impact without adjoint model in an ensemble Kalman filter'. *Quarterly Journal of the Royal Meteorological Society*, 136(651), 1652–1654. https://doi.org/10.1002/qi.658
- Lien, G. Y., Hotta, D., Kalnay, E., Miyoshi, T., & Chen, T. C. (2018). Accelerating assimilation development for new observing systems using EFSO. *Nonlinear Processes in Geophysics*, 25(1), 129–143. https://doi.org/10.5194/npg-25-129-2018
- Lien, G. Y., Kalnay, E., & Miyoshi, T. (2013). Effective assimilation of global precipitation: Simulation experiments. Tellus A: Dynamic Meteorology and Oceanography, 65(1), 19915. https://doi.org/10.3402/tellusa.v65i0.19915
- Liu, J., & Kalnay, E. (2008). Estimating observation impact without adjoint model in an ensemble Kalman filter. Quarterly Journal of the Royal Meteorological Society, 134(634), 1327–1335. https://doi.org/10.1002/qj.280
- Lorenc, A. C., & Marriott, R. T. (2014). Forecast sensitivity to observations in the Met Office Global numerical weather prediction system. Quarterly Journal of the Royal Meteorological Society, 140(678), 209–224. https://doi.org/10.1002/qj.2122
- Maturi, E. (2014). NOAA/NESDIS/STAR GHRSST sea surface temperature products [Dataset]. Zenodo. https://doi.org/10.5281/zenodo.5607102
  Maturi, E., Harris, A., Mittaz, J., Sapper, J., Wick, G., Zhu, X., et al. (2017). A new high-resolution sea surface temperature blended analysis.

  Bulletin of the American Meteorological Society, 98(5), 1015–1026. https://doi.org/10.1175/BAMS-D-15-00002.1
- McDougall, T. J., & Barker, P. M. (2011). Getting started with TEOS-10 and the Gibbs Seawater (GSW) oceanographic toolbox (as latest version v3.05) [Software] (p. 28). SCOR/IAPSO WG127, ISBN 978-0-646-55621-5. Retrieved from https://www.teos-10.org/software.htm
- Ota, Y., Derber, J. C., Kalnay, E., & Miyoshi, T. (2013). Ensemble-based observation impact estimates using the NCEP GFS. *Tellus A: Dynamic Meteorology and Oceanography*, 65(1), 20038. https://doi.org/10.3402/tellusa.v65i0.20038
- Penny, S. G., Akella, S., Buehner, M., Chevallier, M., Counillon, F., Draper, C., et al. (2017). *Coupled data assimilation for integrated Earth system analysis and prediction: Goals, challenges and recommendations.* World Meteorological Organization. WWRP\_2017\_3. Retrieved from https://www.wmo.int/pages/prog/arep/wwrp/new/documents/Final\_WWRP\_2017\_3\_27\_July.pdf
- Penny, S. G., Behringer, D. W., Carton, J. A., & Kalnay, E. (2015). A hybrid global ocean data assimilation system at NCEP. *Monthly Weather Review*, 143(11), 4660–4677. https://doi.org/10.1175/MWR-D-14-00376.1
- Penny, S. G., & Hamill, T. M. (2017). Coupled data assimilation for integrated earth system analysis and prediction. Bulletin of the American Meteorological Society, 98(7), ES169–ES172. https://doi.org/10.1175/bams-d-17-0036.1
- Penny, S. G., Kalnay, E., Carton, J. A., Hunt, B. R., Ide, K., Miyoshi, T., & Chepurin, G. A. (2013). The local ensemble transform Kalman filter and the running-in-place algorithm applied to a global ocean general circulation model. *Nonlinear Processes in Geophysics*, 20(6), 1031–1046. https://doi.org/10.5194/npg-20-1031-2013
- Saha, S., Moorthi, S., Pan, H. L., Wu, X., Wang, J., Nadiga, S., et al. (2010). The NCEP climate forecast system reanalysis [Dataset]. Bulletin of the American Meteorological Society, 91(8), 1015–1058. https://doi.org/10.1175/2010BAMS3001.1
- Saha, S., Moorthi, S., Wu, X., Wang, J., Nadiga, S., Tripp, P., et al. (2014). The NCEP climate forecast system version 2. *Journal of Climate*, 27(6), 2185–2208. https://doi.org/10.1175/jcli-d-12-00823.1
- Sivareddy, S., Paul, A., Sluka, T., Ravichandran, M., & Kalnay, E. (2017). The pre-Argo ocean reanalyses may be seriously affected by the spatial coverage of moored buoys. *Scientific Reports*, 7(1), 1–8. https://doi.org/10.1038/srep46685
- Sluka, T. (2018). Strongly coupled ocean-atmosphere data assimilation with the local ensemble transform Kalman filter (Doctoral Dissertation) (p. 152). University of Maryland. Retrieved from http://hdl.handle.net/1903/22167
- Sriver, R. L., Goes, M., Mann, M. E., & Keller, K. (2010). Climate response to tropical cyclone-induced ocean mixing in an Earth system model of intermediate complexity. *Journal of Geophysical Research*, 115(C10), C10042. https://doi.org/10.1029/2010JC006106

CHANG ET AL. 10 of 11

- Wang, C., Dong, S., & Munoz, E. (2010). Seawater density variations in the North Atlantic and the Atlantic meridional overturning circulation. Climate Dynamics, 34(7), 953–968. https://doi.org/10.1007/s00382-009-0560-5
- Whitaker, J. S., & Hamill, T. M. (2012). Evaluating methods to account for system errors in ensemble data assimilation. *Monthly Weather Review*, 140(9), 3078–3089. https://doi.org/10.1175/MWR-D-11-00276.1
- Winton, M. (2000). A reformulated three-layer sea ice model. *Journal of Atmospheric and Oceanic Technology*, 17(4), 525–531. https://doi.org/10.1175/1520-0426(2000)017<0525;ARTLSI>2.0.CO;2
- Zhang, X., Wang, H., Huang, X. Y., Gao, F., & Jacobs, N. A. (2015). Using adjoint-based forecast sensitivity method to evaluate TAMDAR data impacts on regional forecasts. *Advances in Meteorology*, 2015, 1–13. https://doi.org/10.1155/2015/427616
- Zhu, Y., & Gelaro, R. (2008). Observation sensitivity calculations using the adjoint of the Gridpoint Statistical Interpolation (GSI) analysis system. Monthly Weather Review, 136(1), 335–351. https://doi.org/10.1175/MWR3525.1

## **References From the Supporting Information**

- McDougall, T. J., Jackett, D. R., Millero, F. J., Pawlowicz, R., & Barker, P. M. (2012). A global algorithm for estimating Absolute Salinity. *Ocean Science*, 8(6), 1123–1134. https://doi.org/10.5194/os-8-1123-2012
- Roquet, F., Madec, G., McDougall, T. J., & Barker, P. M. (2015). Accurate polynomial expressions for the density and specific volume of seawater using the TEOS-10 standard. *Ocean Modelling*, 90, 29–43. https://doi.org/10.1016/j.ocemod.2015.04.002

CHANG ET AL. 11 of 11